Inorganic Chemistry

Article

pubs.acs.org/IC

Coordination Polymers Containing Manganese(II)-Azido Layers Connected by Dipyridyl-tetrazine and 4,4′-Azobis(pyridine) Linkers

Paramita Kar,[†] Michael G. B. Drew,[‡] Carlos J. Gómez-García,*[,§] and Ashutosh Ghosh*[,†]

[†]Department of Chemistry, University College of Science, University of Calcutta, 92, A.P.C. Road, Kolkata-700 009, India

[‡]School of Chemistry, The University of Reading, P.O. Box 224, Whiteknights, Reading RG6 6AD, U.K.

[§]Instituto de Ciencia Molecular (ICMol), Parque Científico, Universidad de Valencia, Catedrático José Beltrán, 2. 46980 Paterna, Valencia, Spain

Supporting Information

ABSTRACT: Two new polynuclear manganese(II) complexes $[Mn(dptz)(N_3)_2]_n$ (**1**) and $[Mn(azpy)(N_3)_2]_n$ (**2**) (where dptz = dipyridyl-tetrazine and azpy = 4,4′-azobis-(pyridine)) have been synthesized by self-assembly of the ligand azide, together with dptz and azpy as secondary spacers. The compounds are characterized by single-crystal X-ray diffraction analyses and variable-temperature magnetic measurements. The structural analyses reveal that in complex **1**, which is the first reported Mn(II) complex with the ligand dptz, two $\mu_{1,3}$ bridging azides connect neighboring manganese ions in a zigzag manner to generate a neutral two-dimensional (2D) sheet which is further connected by the dptz ligands to form a three-dimensional (3D) framework. By contrast, complex **2** contains dimeric $[Mn_2(\mu_{1,1}\text{-}N_3)_2]^{2+}$ fragments linked to four identical motifs by means of four single $\mu_{1,3}$-N_3 bridges, that generates a neutral 2D Mn^{II}–azide sheet which is further interconnected by azpy ligands to neighboring manganese ions forming an unprecedented 3D network. Variable-temperature (2–300 K) magnetic susceptibility measurements show the presence of predominantly antiferromagnetic coupling for both complexes that has been reproduced with a regular antiferromagnetic $S = 5/2$ chain (J) with interchain interactions (j) modeled with the molecular field approximation with $J = -7.1$ cm^{-1} and $j' = -0.8$ cm^{-1} for **1** and $J = -4.2$ cm^{-1} and $j' = 0.1$ cm^{-1} for **2**.

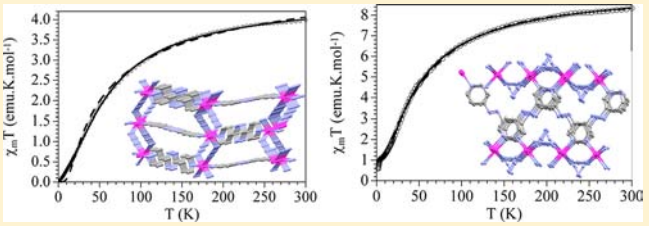

INTRODUCTION

Over the past few years, colossal efforts have been made to develop new high dimensional coordination polymers because of their fascinating structural diversities, their importance in understanding magneto-structural correlations, and their promising potential applications in functional materials.[1] An important strategy to develop polynuclear magnetic materials is to connect the paramagnetic transition metal ions by short bridging ligands which can efficiently mediate the magnetic coupling. Among the used anions, the azide ion is a very popular choice because of its versatile coordinating ability that ranges from $\mu_{1,1}$ (end-on, EO) and $\mu_{1,3}$ (end-to-end, EE) to $\mu_{1,1,1}$, $\mu_{1,1,3}$, $\mu_{1,1,1,1}$, $\mu_{1,1,3,3}$, and $\mu_{1,1,1,3,3,3}$, depending upon the steric and electronic demands of the coligands.[2−4] Moreover, the nature of the magnetic coupling between the metal centers depends upon its coordination modes. For example, EO and EE modes typically mediate ferromagnetic[5] and antiferromagnetic[6] interactions, respectively, although exceptions have been reported.[7] Therefore, one of the most interesting consequences of the coexistence of different bridging modes in the same compound is the formation of various topologies with alternating ferro- and antiferromagnetic interactions.[8] In addition to the short bridging ligands, various types of coligands are used for the construction of such polynuclear complexes, and these coligands play a very important role in controlling the topology and dimensionality of the resulted coordination polymers.[9]

Since long, neutral, N-donor ligands such as pyrazine, 4,4′-bipyridine, bipyrimidine, *trans*-1,2-bis(4-pyridyl)ethylene, 1,4-bis(4-pyridyl)-2,3-diaza-1,3-butadiene, and so forth have been widely used to construct supramolecular architectures along with various anionic species that compensate for the charge of the resulting metal–organic frameworks.[9,10] It is well-known that by a judicious choice of the organic spacer and the central metal ion, it is possible to construct specific architectures with predetermined topologies, connectivities, and even properties. The Mn(II) ion, which is an attractive candidate as a paramagnetic center because of its high $S = 5/2$ value, has been connected by these nitrogen-containing heterocycles along with azide ions by many groups to synthesize coordination polymers of diverse topologies with interesting magnetic properties such as ferro-, antiferro-, and ferrimagnetism, alternating ferro/antiferromagnetism, metamagnetism, spin-canting, spin flop, and so forth.[11] The structure-function relationships of the complexes formed in this way clearly indicate that the bridging modes of the azido groups as well as the nature of the nitrogen containing linkers can play a crucial

Received: November 21, 2012
Published: January 17, 2013

   dx.doi.org/10.1021/ic302548z | *Inorg. Chem.* 2013, 52, 1640−1649

role in determining the overall structure and magnetic properties of the coordination networks. On the other side, the use of long linear coligands constitutes a promising strategy to prepare high dimensional polymeric coordination structures containing cavities or channels (i.e., metal organic frameworks or porous coordination polymers) provided the long ligands adopt a linear disposition.

Herein, we report the synthesis, X-ray single crystal structure analysis, and variable temperature magnetic study of two manganese(II) coordination polymers $[Mn(dptz)(N_3)_2]_n$(**1**) and $[Mn(azpy)(N_3)_2]_n$ (**2**) (where dptz = dipyridyl-tetrazine and azpy = 4,4′-azobis(pyridine), Scheme 1).

Scheme 1. Organic Linkers Used As Pillar

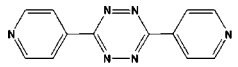

dptz

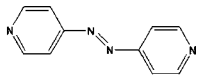

azpy

In compound **1**, $\mu_{1,3}$-N_3 bridging groups connect the neighboring manganese ions in corrugated square grids which are connected by dptz linkers to generate a three-dimensional (3D) structure. In contrast, in compound **2**, the Mn(II) ions form dimers linked by double $\mu_{1,1}$-N_3 bridges that are linked to four identical dimeric entities by means of single $\mu_{1,3}$-N_3 bridges to generate two-dimensional (2D) Mn^{II}-azide sheets which are further interconnected by the azpy ligand to form an unprecedented 3D network. It is to be noted that dipyridyl-tetrazine (dptz) has rarely been used to construct coordination polymers with metal ions. Thus, a search in the Cambridge Crystallographic Data Base (CSD, updated August 2012) shows only 24 metal complexes with the dptz ligand: 11 with Zn, 5 with Cu, 3 with Cd or Ag, and 1 with Ni or Re. Therefore, compound **1** is the first manganese(II) complex with this linker. The azpy ligand has been more often used and thus, the CSD shows almost 200 metal complexes with this ligand although only 10 of them are Mn complexes and only 6 present Mn-azpy-Mn bridges, as observed in compound **2**.

EXPERIMENTAL SECTION

Starting Materials. The reagents and solvents used were of commercially available reagent quality unless otherwise stated and were used without further purification.

Synthesis of the Ligands. 4,4′-Azobis(pyridine) (azpy) and dipyridyl-tetrazine (dptz) were synthesized as orange and purple solids respectively following literature methods.[12]

Caution! *Perchlorate and azide salts of metal complexes with organic ligands are potentially explosive. Only small amounts of material should be prepared and handled with great care.*

Synthesis of $[Mn(dptz)(N_3)_2]_n$(1). An aqueous solution (10 mL) of NaN_3 (2 mmol, 0.130 g) was mixed with a methanolic solution (10 mL) of $Mn(ClO_4)_2{\cdot}6H_2O$ (1 mmol, 0.361 g), and the resulting solution was stirred for 15 min. Dipyridyl-tetrazine(dptz) (1 mmol, 0.236 g) was dissolved in 15 mL of CH_2Cl_2, and this solution was slowly and carefully layered with the Mn(II)-azide solution. Red colored hexagonal shaped single crystals suitable for X-ray diffraction were obtained on the wall of the tube after several days.

Complex **1**: Yield: 0.27 g; 73%. Anal. Calcd. for $C_{12}H_8MnN_{12}$(375.24): C, 38.41; H, 2.15; N, 44.80 Found: C, 38.33; H, 2.09; N, 44.89. IR (KBr pellet, cm^{-1}): 2086 ν(N═N) (bridging azide).

Synthesis of $[Mn(azpy)(N_3)_2]_n$(2). An aqueous solution (10 mL) of NaN_3 (2 mmol, 0.130 g) was added to 5 mL of an aqueous solution of $Mn(ClO_4)_2{\cdot}6H_2O$ (1 mmol, 0.361 g), and the resulting solution was stirred for about 15 min. This solution was slowly and carefully layered with 15 mL of a methanolic solution of azpy (1 mmol, 0.184 g). Orange colored plate-like single crystals suitable for X-ray diffraction were obtained on the wall of the tube after 2−3 weeks.

Complex **2**: Yield: 0.22 g; 67%. Anal. Calcd. for $C_{10}H_8MnN_{10}$(323.20): C, 37.16; H, 2.50; N, 43.34 Found: C, 37.25; H, 2.41; N, 43.23. IR (KBr pellet, cm^{-1}): 2073 ν_{broad}(N═N) (bridging azide), 1593 ν(N═N).

Physical Measurements. Elemental analyses (C, H, and N) were performed using a 2400 series II CHN analyzer. IR spectra in KBr (4500−500 cm^{-1}) were recorded using a Perkin-Elmer RXI FT-IR spectrophotometer. Variable temperature magnetic susceptibility measurements were carried out in the temperature range 2−300 K on polycrystalline samples of the two compounds (with masses of 13.64 and 33.41 mg for compounds **1** and **2**, respectively) using an applied magnetic field of 0.1 T with a Quantum Design MPMS-XL-5 SQUID magnetometer. The isothermal magnetizations were made at 2 K with magnetic fields up to 5 T. The susceptibility data were corrected for the sample holder previously measured using the same conditions and for the diamagnetic contributions of the salt as deduced by using Pascal's constant tables (χ_{dia} = 164.76 × 10^{-6} and −143.54 × 10^{-6} emu.mol^{-1} for **1** and **2**, respectively).

Crystallographic Data Collection and Refinement. A total of 2909 (for **1**) and 3561(for **2**) independent reflection data were collected with MoKα radiation at 293 K using a Bruker SMART diffractometer equipped with a graphite monochromator for **1** and at 150 K using the X-Calibur CCD diffractometer at the University of Reading for **2**. Data analysis for **1** was carried out with the Patterson method by using the SHELXS-97[13] program and for **2** was carried out with the CrysAlis program.[14] The structures were solved using direct methods with the SHELXS-97 program. The non-hydrogen atoms were refined with anisotropic thermal parameters. The hydrogen atoms bonded to carbon were included in geometric positions and given thermal parameters equivalent to 1.2 times those of the atom to which they were attached. Absorption corrections for **1** and **2** were carried out for using the SADABS and ABSPACK programs respectively.[15] Both structures suffered from merohedral twinning so the diffraction patterns were pseudo orthorhombic. The twin ratios were refined with ratios x:1−x with x refining to 0.54(1) in **1** and 0.52(1) in 2. The structures were refined on F^2 to R_1 = 0.0567 and 0.1102 and wR_2= 0.1581 and 0.2943 for 2353, 1368 data with $I > 2\sigma(I)$for **1** and **2**, respectively (Table 1).

RESULTS AND DISCUSSION

Synthesis. Dipyridyl-tetrazine is soluble in dichloromethane but not in methanol or water. When a CH_2Cl_2 solution of dptz was allowed to react with a methanol−water mixture of manganese(II) perchlorate and sodium azide, a red powder of compound **1** was produced immediately by self-assembly. On the other hand, 4,4′-azobis(pyridine) is soluble in methanol. Therefore, for the synthesis of compound **2**, a methanol solution of azpy was added to the water solution of manganese(II) perchlorate and sodium azide. Here also the orange colored powder separated immediately. Both products are sparingly soluble in common organic solvents. So, to obtain single crystals and crystalline compounds, the corresponding linker was dissolved in the solvent as mentioned above and diffused into a methanol−water solution of Mn(II) containing azide anions. It may be noted that both compounds **1** and **2** have the same metal to ligand ratios (1:2) and possess 3D frameworks, but the bridging mode of the azido ligand and the topology of the frameworks are very different (see description of structures below).

IR Spectra of the Complexes. Spectroscopic data and their assignments are given in the Experimental Section. Assignments are based on the structures of **1** and **2** and related complexes previously reported.[16] The coordination mode of

dx.doi.org/10.1021/ic302548z | Inorg. Chem. 2013, 52, 1640−1649

Table 1. Crystal Data and Structure Refinement of Complexes 1 and 2

	1	2
formula	$C_{12}H_8MnN_{12}$	$C_{10}H_8MnN_{10}$
formula weight	375.24	323.20
space group	$P2_1/n$	$P2_1/c$
crystal system	monoclinic	monoclinic
a/ Å	7.426(5)	9.933(4)
b/ Å	21.307(14)	9.1087(16)
c/ Å	9.324(6)	14.479(4)
β/deg	90.127(7)	91.352(7)
V/Å^3	1475.3(17)	1309.7(7)
Z	4	4
calculated density D_{calc}/g cm^{-3}	1.689	1.639
absorption coeff.(μ) mm^{-1}	(Mo Kα) 0.921	(Mo Kα) 1.019
F(000)	756	652
crystal size (mm)	0.05 × 0.05 × 0.30	0.07 × 0.07 × 0.26
θ range (deg)	1.0 to 26.9	2.6 to 30.0
R(int)	0.048	0.125
no of data measured	10095	6479
no. of unique data	2909	3561
data with $I > 2\sigma(I)$	2353	1368
R1, wR2	0.0567, 0.1581	0.1102, 0.2943
residual electron density(e A^{-3})	0.542, −0.605	0.962, −1.380

azide to transition metal is usually detected by the IR band due to $\nu_{as}(N_3)$ which occurs above 2000 cm^{-1}. In general, it appears around 2055 cm^{-1} for the bridging azide and below 2055 cm^{-1} for the terminal ion. In the spectrum of complex **1**, a sharp and strong band at 2086 cm^{-1} is indicative of the presence of the bridging azide whereas a broad band at around 2073 cm^{-1} for complex **2** corroborates the presence of two types of bridging modes of azido ligands ($\mu_{1,1}$ and $\mu_{1,3}$ bridges). In complex **1**, one single, sharp and strong band at 1390 cm^{-1}, indicates the presence of dptz. Compound **2** exhibits one single, sharp and strong band at 1593 cm^{-1}, attributable to the presence of the N═N stretch vibration of the azpy ligand.

Description of Structures of Complexes 1 and 2. Complex **1** is a 3D coordination polymer built by inorganic layers connected by the organic dptz ligand. The inorganic layers are formed by Mn(II) ions bridged by single $\mu_{1,3}$ azido bridges. The asymmetric unit of complex **1** contains one Mn(II) atom, one dptz ligand, and two azide ions as depicted in Figure 1.

The Mn(II) atoms assume a distorted octahedral geometry being bonded to four $\mu_{1,3}$ bridging azido groups together with two trans nitrogen atoms from the two dptz ligands. The four azido nitrogen atoms (N1, N3′, N4, and N6″(symmetry codes ′ = x − 0.5, 0.5 − y, z + 0.5, ″ = x + 0.5, 0.5 − y, z + 0.5)), constitute the equatorial plane with Mn−N distances ranging from 2.202(5) to 2.249(5) Å while the pyridyl nitrogens (N11 and N21) from dptz ligands coordinate in *trans* axial positions with slightly elongated Mn−N distances of 2.276(4) and 2.266(4) Å, respectively. Selected bond lengths and angles are summarized in Table 2.Thus, each Mn(II) is connected to four neighbors via single $\mu_{1,3}$ azido bridges, yielding a neutral 2D (4,4) Mn(II)azido-based quadratic layer parallel to the *ac* plane (Figure 2a).

Table 2. Bond Distances (Å) and Angles (deg) in the Metal Coordination Sphere of Complex 1[a]

Bond Distances (Å)	
Mn(1)−N(1)	2.249(5)
Mn(1)−N(3)′	2.202(5)
Mn(1)−N(4)	2.235(5)
Mn(1)−N(6)″	2.213(5)
Mn(1)−N(11)	2.276(4)
Mn(1)−N(21)	2.266(4)
Bond Angles (deg)	
N(3)′−Mn(1)−N(6)″	90.5(2)
N(3)′−Mn(1)−N(4)	89.8(2)
N(6)′−Mn(1)−N(4)	175.9(2)
N(3)′−Mn(1)−N(1)	174.6(3)
N(6)−Mn(1)−N(1)	91.4(2)
N(4)−Mn(1)−N(1)	88.0(2)
N(3)′−Mn(1)−N(21)	93.9(2)
N(6)″−Mn(1)−N(21)	92.3(3)
N(4)−Mn(1)−N(21)	91.8(2)
N(1)−Mn(1)−N(21)	91.1(2)
N(3)′−Mn(1)−N(11)	89.1(2)
N(6)″−Mn(1)−N(11)	86.9(2)
N(4)−Mn(1)−N(11)	88.9(2)
N(1)−Mn(1)−N(11)	85.9(2)
N(21)−Mn(1)−N(11)	176.9(2)

[a]Symmetry elements: ′ = x − 0.5, 0.5 − y, z + 0.5, ″ = x + 0.5, 0.5 − y, z + 0.5.

The Mn−N−(N)−N−Mn torsion angles are 75.5° and 61.3°, and the Mn−Mn distances spanned by the $\mu_{1,3}$-N_3 bridges are 6.077(2) and 6.065(2) Å, respectively. Adjacent azido bridged Mn atoms are related by 2-fold screw axes leading to a systematic alternation of slanted coordination polyhedra throughout the layer: the equatorial plane of each Mn(II) ion makes a dihedral angle of 40.5° with the plane formed by the Mn(II) ions in the layer. The equatorial planes of neighboring Mn(II) ions are almost orthogonal with a dihedral angle of 86.74°. The systematic alternation in coordination orientation

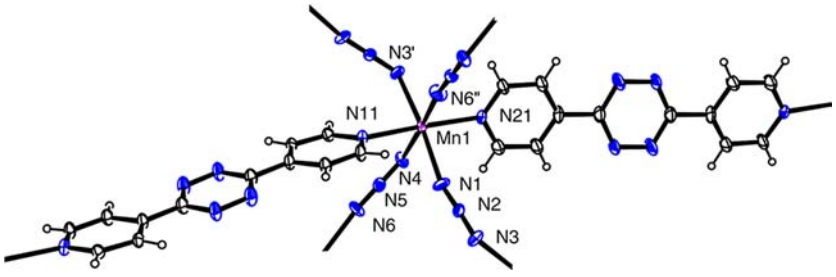

Figure 1. Coordination environment of the Mn(II) ion in the structure of **1** with ellipsoids at 30% probability. Symmetry codes ′ = x − 0.5, 0.5 − y, z + 0.5, ″ = x + 0.5, 0.5 − y, z + 0.5.

dx.doi.org/10.1021/ic302548z | Inorg. Chem. 2013, 52, 1640−1649

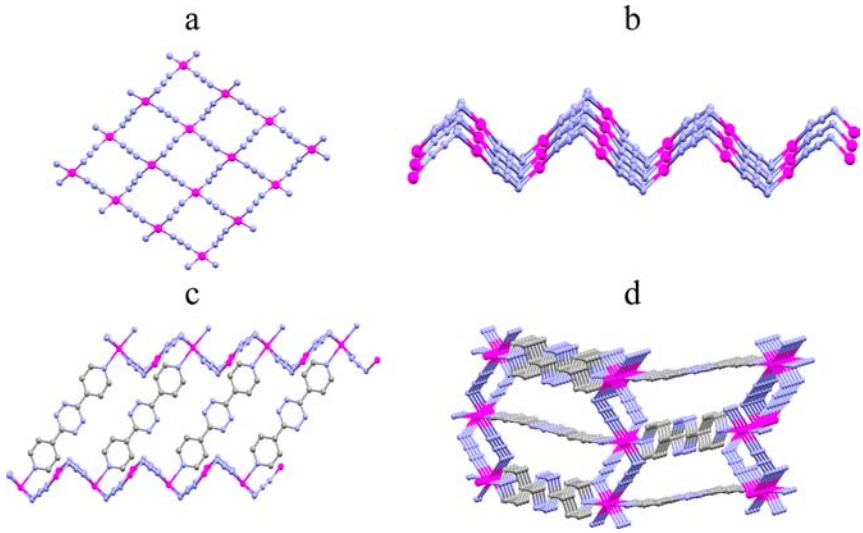

Figure 2. Structure of compound **1**: (a) Projection of the square sheet formed by $\mu_{1,3}$ azido bridged Mn(II) ions; (b) Side view showing the undulating shape of the layer; (c) Pillaring of the inorganic layers in a concave-to-convex mode and (d) 3D framework resulting from the connection of the square sheets by the dptz molecules.

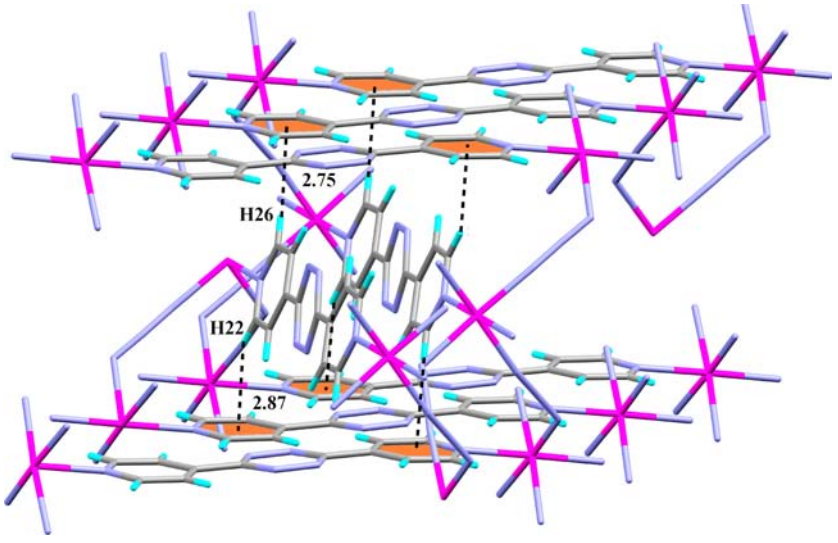

Figure 3. Stabilization of the 3D framework in **1** by CH---π supramolecular interactions.

leads to the undulating shape for the manganese(II) azido layer depicted in Figure 2b.

The inorganic layers are connected by the linear organic dptz spacers in a concave-to-convex mode (Figure 2c) to generate a hybrid 3D architecture (Figure 2d). The spacers are arranged almost orthogonally with respect to the two neighboring azido bridged Mn(II). The Mn−Mn distance through the pillar ligands (15.56 Å) is much longer than the interlayer separation (10.653 Å) and the shortest interlayer Mn−Mn distance (9.497 Å).

Although there are no significant π-stacking interactions between aromatic rings in **1**, there are several edge-to-face intermolecular C−H···π interactions between the pyridine rings disposed approximately perpendicular to the adjacent pyridyl rings of neighboring dptz ligands (Figure 3). The distance between H22 and the centroid of the pyridine ring of adjacent dptz moieties is 2.87 Å and the C22−H22···Cg angle is 159°, whereas, the distance between H26 and the centroid of the pyridine ring of adjacent dptz moieties is 2.75 Å and the C26−H26···Cg angle is 147°. [Cg = centroid of the pyridine ring (N(11)−C(12)−C(13)−C(14)−C(15)−C(16)].

A CSD search shows that only 9 manganese(II) azido compounds containing single $\mu_{1,3}$ azido-bridged (4,4) layers have been reported to date. Six of these nine are 3D pillared-layer networks with pyrimidine(pym),[17] pyrazine-*N*,*N*′-dioxide-(pzdo),[11c] 4-pyridylmethylketazine (4-pmk),[11d] two with 4,4′-bipy,[18] and *N*,*N*′-bis-(1-pyridin-4-yl-ethylidene)-hydrazine (hyd)[19] as pillars. The undulating 2D layer in **1** is very similar to those observed in the 2D compounds $[Mn(4\text{-acpy})_2(N_3)_2]_n$,[11a] $Mn(N_3)_2(btr)_2$,[20] and $[Mn(minc)_2(N_3)_2]_n$[11e] (4-acpy = 4-acetylpyridine, minc = methyl isonicotinate, btr = 4,4′-bi-1,2,4-triazole) and the 3D polymers $[Mn(4,4'\text{-bipy})(N_3)_2]_n$,[18] $[Mn(pym)(N_3)_2]_n$,[17] $[Mn(4\text{-pmk})(N_3)_2]_n$,[11d] $Mn(N_3)_2(pzdo)$[11c] and $[Mn(hyd)(N_3)_2]_n$.[19] Among these 3D polymeric structures, the complexes with 4,4′-bipy[18] exhibit two topologically and magnetically different metal organic frameworks (MOFs): one is a $\mu_{1,3}$ azido bridged 3D manganese(II) lattice with bridging 4,4′-bipyridine ligands

dx.doi.org/10.1021/ic302548z | *Inorg. Chem.* 2013, 52, 1640−1649

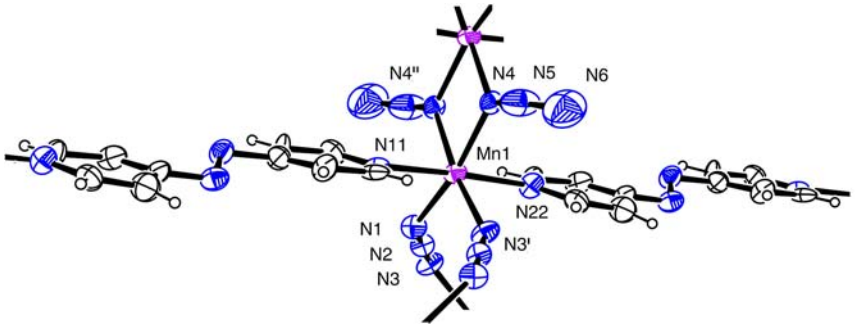

Figure 4. Coordination environment of the Mn(II) ion in the structure of **2** with ellipsoids at 30% probability.(Symmetry codes: ′ = 1 − *x*, 0.5 + *y*, 0.5 − *z*, ″ = 1 − *x*, −*y*, 1 − *z*).

and the second is an acentric 3D structure where Mn(II) ions are linked through $\mu_{1,3}$-azido groups resulting in a diamond-like network. The former is structurally similar to that of **1**. The pzdo, 4-pmk, pym, and hyd-based structures produce a similar topological network to that of compound **1** but with a significant change in the interlayer distance although the interlayer stacking mode and net topology remain the same.

Complex **2** is also a 3D coordination polymer built by the organic azpy ligand interlinking 2D inorganic layers in which doubly $\mu_{1,1}$ azido-bridged dimanganese(II) units are joined by single $\mu_{1,3}$ azido bridges. The asymmetric unit consists of one Mn(II) ion, one azpy ligand, and two azide ions (one $\mu_{1,3}$ and one $\mu_{1,1}$). The Mn(II) coordination environment of compound **2** is similar to that of **1**: an elongated octahedron formed by four azido ligands in the equatorial positions (with Mn−N bond lengths in the range 2.159(8)−2.189(8) Å) and two trans N atoms from azpy ligands in the axial positions with Mn−N bond lengths of 2.258(9) and 2.291(9) Å (Figure 4). The two pyridine rings of the azpy ligands are approximately coplanar, with a dihedral angle of 3.5(3)°.The relevant bond parameters are collected in Table 3.

In the Mn(II) dimers, the two metals are symmetry related over an inversion center and bridged by two $\mu_{1,1}$-azides though N4 and N4′ as shown in Figures 4 and 5a. In the Mn_2N_2 planar ring, the Mn−N−Mn bridging angle is 103.94(3)° and the Mn···Mn distance is 3.448(2) Å. Each dimeric $[Mn_2(\mu_{1,1}\text{-}N_3)_2]^{2+}$ fragment is linked to four identical dimers by means of single $\mu_{1,3}$ azido bridges generating a neutral 2D Mn^{II}-azide sheet (Figures 5b and 5c). The layers are parallel to the *bc* plane and exhibit a three-connected (6,3) topology, with Mn atoms as nodes and both double $\mu_{1,1}$ and single $\mu_{1,3}$ azido bridges as linkers. The Mn···Mn distance along the $\mu_{1,3}$-N_3 bridge is 5.935(3) Å, and the Mn−N−N−N−Mn torsion angle is 70.2°. The layer structure may also be described as consisting of single $\mu_{1,3}$ azido-bridged Mn(II) helical chains interlinked by double $\mu_{1,1}$ azido bridges. The helical chains twist around 2-fold screw axes along the *c* direction. The helicity leads to a systematic alternation of two different orientations of the Mn(II) coordination spheres along the chain resulting in an almost orthogonal orientation of the equatorial planes of the neighboring Mn(II) centers linked by single $\mu_{1,3}$ azido bridges (with a dihedral angle of 83.1°). This alternation also results in an almost orthogonal orientation on the Mn_2N_2 planar rings of adjacent dimers (dihedral angle of 81.1°) leading to an undulating inorganic layer (Figure 5d).

The 2D inorganic layers are connected by azpy ligands to form a 3D inorganic−organic hybrid coordination network (Figures 5e and 5f). These azpy ligands adopt a nearly planar transoid conformation and connect Mn(II) ions from neighboring layers with a Mn···Mn distance of 13.477 Å, significantly longer than the interlayer separation (9.929 Å), defined as the distance between the mean Mn(II) planes of neighboring layers. In contrast to compound **1**, the undulating inorganic layers are stacked in a concave-to-concave mode (Figure 5e). The 3D framework is further stabilized by two types of face to face $\pi-\pi$ interactions between the pyridine rings of the spacer azpy molecules (see Figure 6a): first between pyridine rings of azpy ligands connecting Mn(II) ions of the same dimer and second between different dimers with centroid−centroid distances of 3.627(6) and 3.642(6) Å, respectively. These $\pi-\pi$ interactions are quite strong, as shown by the dihedral angles between the rings (3.5° and 16.7°, respectively) and the slip angles (16.1° and 7.9°, respectively).

Although metal azido layers with alternate double $\mu_{1,1}$ and single $\mu_{1,3}$ azido bridges have been found in ten different Mn(II) compounds, a detailed search in the CSD database shows that only five of these ten compounds present a bridging pattern of the inorganic metal-azide layer similar to that of

Table 3. Bond Distances (Å) and Angles (deg) in the Metal Coordination Sphere of Complex 2[a]

Bond Distances (Å)	
Mn(1)−N(1)	2.175(9)
Mn(1)−N(3)′	2.159(8)
Mn(1)−N(4)	2.189(7)
Mn(1)−N(4)″	2.189(8)
Mn(1)−N(11)	2.291(9)
Mn(1)−N(22)‴	2.258(9)
Bond Angles (deg)	
N(1)−Mn(1)−N(3)′	98.6(3)
N(1)−Mn(1)−N(4)	166.0(3)
N(3)′−Mn(1)−N(4)	95.4(4)
N(1)−Mn(1)−N(4)″	90.0(3)
N(3)′−Mn(1)−N(4)″	171.3(4)
N(4)−Mn(1)−N(4)″	76.1(3)
N(1)−Mn(1)−N(11)	88.3(3)
N(3)′−Mn(1)−N(11)	89.4(3)
N(4)−Mn(1)−N(11)	91.8(3)
N(4)″−Mn(1)−N(11)	92.7(3)
N(1)−Mn(1)−N(22)‴	91.5(3)
N(3)′−Mn(1)−N(22)‴	86.7(3)
N(4)−Mn(1)−N(22)‴	89.4(3)
N(4)″−Mn(1)−N(22)‴	91.3(3)
N(11)−Mn(1)−N(22)‴	176.0(3)

[a]Symmetry elements: ′ = 1 − *x*, 0.5 + *y*, 0.5 − *z*, ″ = 1 − *x*, −*y*, 1 − *z*, ‴ = −1 + *x*, −1 + *y*, *z*.

dx.doi.org/10.1021/ic302548z | *Inorg. Chem.* 2013, 52, 1640−1649

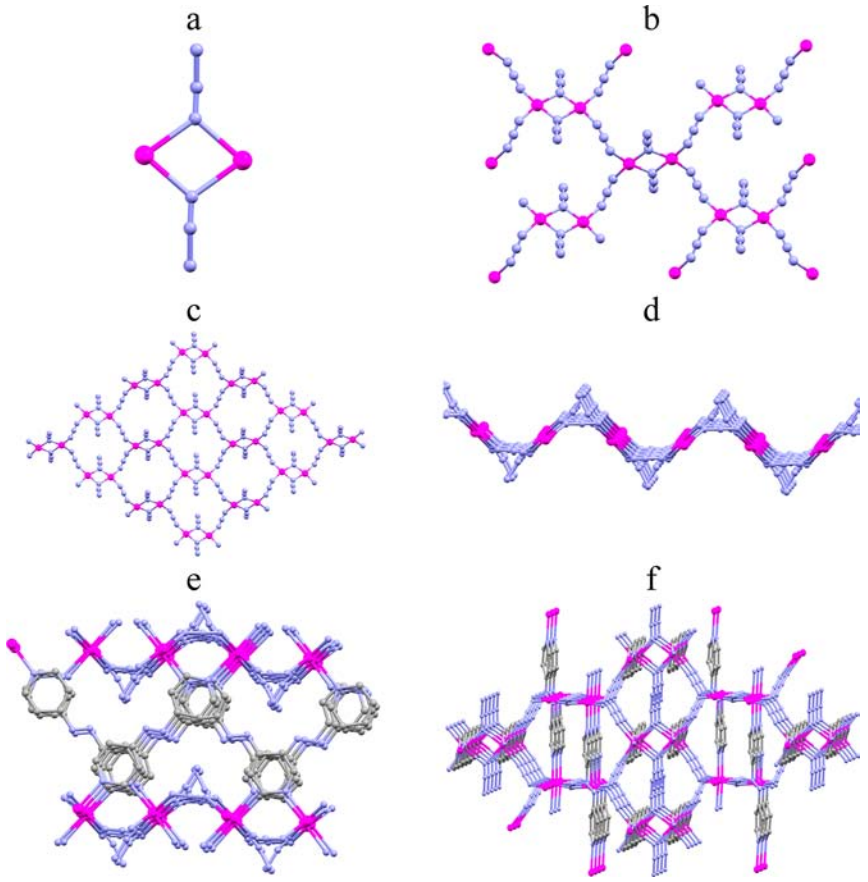

Figure 5. (a) $\mu_{1,1}$ azido-bridged dimeric cationic unit $[Mn_2(\mu_{1,1}\text{-}N_3)_2]^{2+}$; (b) Connection of the $[Mn_2(\mu_{1,1}\text{-}N_3)_2]^{2+}$ fragments to four identical dimers by means of single $\mu_{1,3}$-azido bridges. (c) Top view and (d) Side view of the neutral (6,3) 2D Mn(II)-azido sheets. (e) Side view of the Mn-azido layers showing the azpy ligands connecting the layers in a concave-to-concave mode, and (f) Top view of the 3D framework showing the layers connected by the azpy ligands.

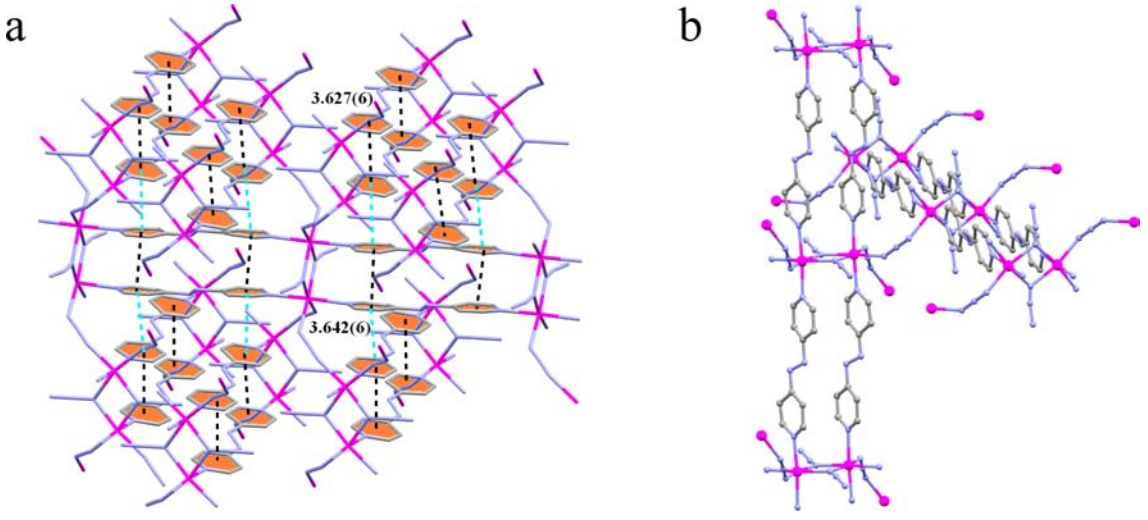

Figure 6. (a) Supramolecular $\pi-\pi$ interactions between the pyridine rings of the pillar ligands. (b) Perpendicular arrangement of the pillars connecting Mn(II) of different dimers in complex **2**.

compound **2** in which doubly $\mu_{1,1}$-N_3 bridged dimers are connected to four neighboring dimers through single $\mu_{1,3}$-N_3 bridges. Three of these are 3D networks containing *N*-methyl-4-pyridinium tetrazolate (mptz),[21] bipyrimidine (bpym),[22] and *N*,*N*′-bis-(1-pyridin-4-yl-ethylidene)-hydrazine (hyd)[19] spacers respectively. The remaining complexes are 2D or 1D.[23] Among the three 3D structures, in those containing mptz[21] and bpym,[22] the hybrid inorganic−organic 2D layers containing the $\mu_{1,1}$-N_3 and the organic ligands are further connected by $\mu_{1,3}$-N_3 bridges to construct the 3D framework and, therefore, only in the compound containing *N*,*N*′-bis-(1-pyridin-4-yl-ethylidene)-hydrazine)[19] does the coligand act as a pillar between the 2D Mn-azido inorganic layers to form a 3D network, as observed in **2**. However, in this last example, the pillars connecting adjacent

dx.doi.org/10.1021/ic302548z | *Inorg. Chem.* 2013, 52, 1640−1649

Mn(II) ions of neighboring dimers are parallel whereas in **2** they are perpendicular (Figures 5e and 6b), thus, giving rise to an unprecedented topology.

Magnetic Properties. The product of the molar magnetic susceptibility times the temperature ($\chi_m T$) per Mn(II) ion for compound **1** shows a room temperature value of about 4.0 emu K mol^{-1}, slightly below the expected value of 4.375 emu K mol^{-1} for one isolated Mn(II) ion with g = 2 . When cooling down the sample, the $\chi_m T$ product shows a progressive and continuous decrease to reach a value of about 0.05 emu K mol^{-1} at 2 K (Figure 7). This behavior indicates the presence of predominantly antiferromagnetic interactions between the Mn(II) ions in compound **1**.

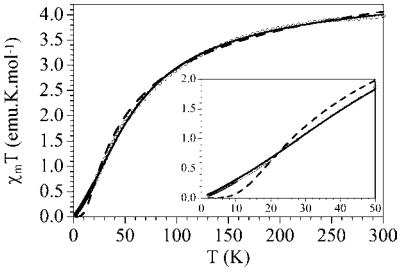

Figure 7. Thermal variation of the $\chi_m T$ product per Mn(II) ion for compound **1**. Solid and dashed lines represent the best fit to the models (see text).

Although the structure of compound **1** presents a 3D network, we can consider that the magnetic coupling through the long pillars connecting the Mn-azido layers is negligible. Once this interaction is removed, the structure of compound **1** consists of a rectangular 2D layer where each Mn(II) ion is connected to four different Mn(II) ions through two different $\mu_{1,3}$-N_3 bridges (N1−N2−N3 and N4−N5−N6) in opposite directions. Accordingly, as a first approximation, we create two different models: (i) a square 2D lattice, if we consider that the two azido bridges are similar, and (ii) a rectangular 2D lattice modeled by a regular linear chain with interchain interactions, if we consider that the two azido bridges are different. Thus, for the first structure, we fitted the magnetic properties of compound **1** with a S = 5/2 quadratic layer antiferromagnet (QLAF) model.[24] This model reproduces quite well the magnetic properties of compound **1** with the following parameters: g = 2.0 (fixed value) and J = −2.8 cm^{-1} (dashed line in Figure 7). However, in the low temperature region the agreement between the experimental data and the model is not so good (inset in Figure 7). The second model (a regular S = 5/2 chain[25] with interchain interactions modeled with the molecular field approximation)[26] gives a much better agreement in the whole temperature range with the following parameters: g = 2.0 (fixed value), J = −7.1 cm^{-1} and j = −0.8 cm^{-1}, (solid line in Figure 7) (all the Hamiltonians are written as H = $-J\sum S_i S_{i+1}$).

The $\chi_m T$ product per Mn(II) dimer of compound **2** shows at room temperature a value of about 8.3 emu K mol^{-1}, close to the expected value of 8.75 emu K mol^{-1} for two noninteracting Mn(II) ions. When cooling down the sample, $\chi_m T$ shows a continuous and progressive decrease to reach a plateau between about 8 and 4 K with a value of about 1.0 emu K mol^{-1}. Below about 4 K $\chi_m T$ shows a more abrupt decrease to reach a value of about 0.6 emu K mol^{-1} at 2 K (Figure 8). This behavior indicates, as in compound **1**, the presence of predominantly antiferromagnetic interactions between the Mn(II) ions.

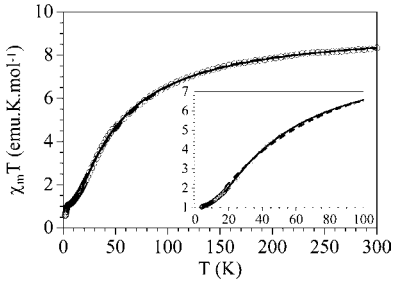

Figure 8. Thermal variation of the $\chi_m T$ product per Mn(II) dimer for compound **2**. Solid and dashed lines represent the best fit to the models (see text).

Compound **2** presents a 2D layer formed by Mn(II) dimers presenting a double $\mu_{1,1}$-N_3 bridge which are further connected with four other dimers through single $\mu_{1,3}$-N_3 bridges. If we assume that the $\mu_{1,3}$-N_3 bridges give a larger (antiferro)-magnetic coupling, from the magnetic point of view, compound **2** can also be considered as a regular zigzag Mn(II) chain with intrachain $\mu_{1,3}$-N_3 bridges that are further connected through interchain double $\mu_{1,1}$-N_3 bridges. Accordingly, we have fitted the magnetic properties of compound **2** with two different models: (i) a S = 5/2 dimer with interdimer interactions modeled with molecular field approximation[26] and (ii) a regular S = 5/2 chain[25] with interchain interactions also modeled with the molecular field approximation.[26] The first model, a dimer with interdimer interactions, reproduces very satisfactorily the magnetic properties of compound **2** in the 10−300 K temperature range with the following parameters: g = 2.0 (fixed value), J_{dim} = 13.5 cm^{-1} and j'_{dim} = −3.9 cm^{-1} (J_{dim} and j'_{dim} are the intra- and interdimer exchange interactions, respectively, dashed line in Figure 8). The second model, a regular chain with interchain interactions, reproduces the magnetic properties of compound **2** slightly better than the first model with the following parameters: g = 2.0 (fixed value), J_{chain} = −4.2 cm^{-1}, and j'_{chain} = 0.1 cm^{-1}, where J_{chain} and j'_{chain} are the intra- and interchain exchange interactions, respectively, solid line in Figure 8. Note that below about 10 K the sample presents a plateau at about 1.0 emu K mol^{-1} that suggests the presence of a paramagnetic impurity. To obtain more reliable parameters, we have not included the low temperature data (T < 10 K) in the fitting procedure.

As expected, the first model is not as good as the second (inset in Figure 8) and gives less realistic parameters (J_F> $|J_{AF}|$), since the antiferromagnetic coupling through the $\mu_{1,3}$-N_3 bridge has to be bigger in absolute value than the ferromagnetic coupling through the $\mu_{1,1}$-N_3 bridge.

In both compounds the predominantly antiferromagnetic couplings are also confirmed by the isothermal magnetization at 2 K that shows a residual signal due to the presence of a small fraction of paramagnetic impurities and a linear behavior with no saturation at 5 T.

The antiferromagentic coupling found in compound **1** is easy to rationalize if we consider the magneto structural correlations and theoretical calculations that predict a moderate antiferromagnetic Mn(II)−Mn(II) coupling for single $\mu_{1,3}$-N_3 bridges.[27] These correlations establish that, besides the Mn−N bond distance, the main parameters determining the magnetic coupling are the Mn−N−N bond angles (β) and

dx.doi.org/10.1021/ic302548z | Inorg. Chem. 2013, 52, 1640−1649

Table 4. Bond Angles (deg) and Lengths (Å) and Magnetic Parameters of All the Mn(II)-azide Compounds Containing Double $\mu_{1,1}$-N_3 and Single $\mu_{1,3}$-N_3 Bridges[a]

compound	Mn−$N_{1,1}$-Mn	Mn−$N_{1,1}$	Mn−$N_{1,3}$-N	Mn−$N_{1,3}$	$J_{1,1}$ (cm^{-1})	$J_{1,3}$ (cm^{-1})	ref
CAKWUI	101.7	2.277	146.4	2.174	0.99	−5.91	21
		2.323	138.2	2.178			
CUCDUZ	101.4	2.207	150.5	2.164	3.3	−5.16	23a
		2.262					
CUCHEN	99.6	2.214	133.1	2.188	2.3	−6.01	23a
		2.280					
FEWRAB	99.7	2.230	125.2	2.205	>0	<0	11g
		2.231	137.9	2.180			
			167.5	2.185			
			127.2	2.202			
GACTUA[b]	96.5	2.209	146.5	2.127			23b
		2.289	137.6	2.169			28
GACVAI[b]	96.2	2.224	130.4	2.134			23b
		2.269	140.8	2.180			28
HOTDAV	102.2	2.203	153.9	2.223	1.7	−5.4	23c
		2.337	163.8	2.147			
IPAYEE[c]	120.3[d]	2.210	144.2	2.205			23d
	95.4	2.319					
	95.5	2.277					
		2.358					
		2.233					
IPAYOO[c]	103.8	2.189	128.0	2.309			23d
	101.4	2.238	144.9	2.238			
		2.174					
		2.220					
NAJTIB	104.5	2.215	161.3	2.177	>0	<0	22
		2.230	126.6	2.216			
2	103.9	2.188	136.3	2.176	0.1	−4.2	this work
		2.189	145.9	2.158			

[a]Only compounds CAKWUI, GACTUA, GACVAI, HOTDAV, and NAJTIB present the same topology as compound **2**. [b]Besides the double $\mu_{1,1}$-N_3, there is an additional −N-N- bridge in the Mn(II) dimer [c]Besides the double $\mu_{1,1}$-N_3, there is an additional −OCO- bridge in the Mn(II) dimer [d]This angle corresponds to the single intertrimer $\mu_{1,1}$-N_3 bridge

the torsion angle (τ) between the average planes formed by the N_3^- anion with each of the two Mn(II) ions. Thus, antiferromagnetic coupling is expected to be maximum for low β values (ca. 110°) and minimum for higher β values (ca. 160°). On the other hand, the correlations with the torsion angle (τ) indicate that, as expected, the larger this angle, the larger the antiferromagnetic coupling, since the Mn−N_3−Mn unit is closer to planarity. With these correlations in mind, although it is not straightforward, we can try to assign the different coupling constants (J_{chain} = −7.1 cm^{-1} and j'_{chain} = −0.8 cm^{-1}) to each of the two $\mu_{1,3}$-N_3 bridges present in **1**. Careful examination of the bond distances and angles in both bridges show that, although the Mn−N average bond distances are the same (2.225 Å), one of the Mn−N−N bond angles and the Mn−N−N−N dihedral angles are different. Thus, although the Mn−N3−N2 and Mn−N4−N5 bond angles are very similar (125.1(4)° and 125.0(4)°, respectively), the two other Mn−N−N angles, Mn−N1−N2 and Mn−N6−N5, are different (166.1(6)° and 172.2(6)°, respectively). Since the magnetic coupling is limited by the lowest of the two magnetic couplings across the bridge, we can expect that the largest angle, which provides the lowest coupling, should be the limiting parameter in determining the J value. This assumption implies that, since the Mn−N1−N2 angle (166.1°) is closer to 160°, where the coupling is minimum, this bridge should give the lower coupling constant and, therefore we assign the −0.8 cm^{-1} interchain coupling to the −N1−N2−N3− bridge and the larger one (−7.1 cm^{-1}) to the −N4−N5−N6− bridge. Furthermore, the dihedral angles between the average planes containing the Mn atoms and the three N atoms, (97.3, 144.0° respectively for the N1−N2−N3 N4−N5−N6 bridge, also point in this direction since the dihedral angle across the −N4−N5−N6− bridge is closer to linearity and, therefore, it is expected to give a higher magnetic coupling. Note that the two J values found in compound **1** are within the typical values found in other $\mu_{1,3}$-N_3 bridges connecting Mn(II) ions.[11e,21−23,26,28]

The magnetic behavior of compound **2** is also quite easy to rationalize since double $\mu_{1,1}$-N_3 bridges are well-known to produce ferromagnetic coupling when the Mn−N−Mn bond angles are above about 98°.[29] Since in compound **2** the Mn−N−Mn bond angle is 103.9(3)°, we expect a ferromagnetic coupling through this double $\mu_{1,1}$-N_3 bridge in agreement with the experimental results. For the single $\mu_{1,3}$-N_3 bridge, as discussed above, the magnetic coupling is always moderate to strong antiferromagnetic, and the magnitude depends on the Mn−N−N bond angle (β) and the torsion angle (τ) in the Mn−N−N−N−Mn bridge. In compound **2** the β angles are 145.9° and 136.3° implying that the magnetic coupling should be higher than that observed in compound **1**, where the angles are closer to 160°. Albeit, among the other parameters determining the coupling, the dihedral angle τ (69.0° in

dx.doi.org/10.1021/ic302548z | Inorg. Chem. 2013, 52, 1640−1649

compound **2**) is much lower than the corresponding values in compound **1** (97.3° and 144.0°) and, therefore, the magnetic coupling is expected to be much lower since the orbital overlap is worse. These two opposite parameters lead to a J value in compound **2** (J = −4.2 cm^{-1}) which is intermediate between the two J values found in compound **1** (−7.1 and −0.8 cm^{-1}).

As observed in compound **1**, the J value observed in **2** is in between the normal range observed for this type of $\mu_{1,3}$-N_3 single bridge.[11e,21−23,26,28] A detailed search in the CSD database shows up to ten different Mn(II) compounds presenting both double $\mu_{1,1}$-N_3 and single $\mu_{1,3}$-N_3 bridges (Table 4). Five of these ten compounds present a similar bridging pattern to that of compound **2**, thus containing doubly $\mu_{1,1}$-N_3 bridged dimers connected to four neighboring dimers through single $\mu_{1,3}$-N_3 bridges. The only two of these five examples that have been magnetically characterized show very similar magnetic couplings, and the three remaining examples present an overall antiferromagnetic behavior although no J values were provided. As can be seen in Table 4, in all the magnetically characterized examples, the $\mu_{1,1}$-N_3 bridge gives weak ferromagnetic couplings whereas the $\mu_{1,3}$-N_3 bridges give antiferromagnetic couplings with higher absolute values.

CONCLUSIONS

The use of Mn(II) and azido anions together with long pillaring coligands, dipyridyl-tetrazine (dptz) or 4,4′-azobis(pyridine) (azpy), has allowed the synthesis of two novel 3D structures in which the layered Mn(II)-azido bridged lattices are further connected by the long dptz or azpy ligands. Although in the present cases the long pillaring ligands that connect the layers are not orthogonal to the layers but tilted, resulting in a significant reduction of the interlayer space, the use of similar pillaring ligands containing functional groups in the pyridine rings, especially in the 2-position is expected to preclude this tilted orientation in favor of the perpendicular one, and thus should lead to MOFs with a larger void volume in the interlayer space. The magnetic properties of compound **1**, one of the few characterized examples of a Mn(II) rectangular antiferromagnetic lattice, can be very well reproduced with a simple regular antiferromagnetic chain model including interchain interactions (also antiferromagnetic), as expected for $\mu_{1,3}$-N_3 bridges. The known magneto-structural correlations for this kind of bridge have allowed us to assign the two coupling constants to the two different $\mu_{1,3}$-N_3 bridges present in **1**. Compound **2** with its unprecedented topology, is one of the few known examples of a $\mu_{1,1}$-N_3 doubly bridged Mn(II) dimer connected to four other dimers through simple $\mu_{1,3}$-N_3 bridges. Its magnetic properties have been reproduced with an antiferromagnetic regular chain model, as for compound **1**, although now the interchain interactions, representing the coupling through the double $\mu_{1,1}$-N_3 bridge, are, as expected, weak and ferromagnetic. Compound **1** is the first reported manganese complex with the dptz ligand.

ASSOCIATED CONTENT

Supporting Information

Crystallographic data in CIF format. This material is available free of charge via the Internet at http://pubs.acs.org.

AUTHOR INFORMATION

Corresponding Author

*E-mail: carlos.gomez@uv.es (C.J.G.-G.), ghosh_59@yahoo.com (A.G.).

Notes

The authors declare no competing financial interest.

ACKNOWLEDGMENTS

P.K. is thankful to CSIR, India, for research fellowship [Sanction no. 09/028(0733)/2008-EMR-I]. We thank EPSRC and the University of Reading for funds for the X-Calibur CCD Diffractometer and the DST-FIST, India-funded Single Crystal Diffractometer Facility at the Department of Chemistry, University of Calcutta. We thank the Spanish Ministerio de Economía y Competitividad (Projects Consolider-Ingenio in Molecular Nanoscience CSD2007-00010 and CTQ-2011-26507) and the Generalitat Valenciana (Projects Prometeo 2009/95 and ISIC). Thanks are given to the Consejo Superior de Investigaciones Científicas (CSIC) of Spain for the award of a license for the use of the Cambridge Crystallographic Data Base (CSD).

REFERENCES

(1) (a) Qiu, S.; Zhu, G. *Coord. Chem. Rev.* **2009**, *253*, 2891−2911. (b) Chelebaeva, E.; Larionova, J.; Guari, Y.; SaFerreira, R. A.; Carlos, L. D.; Paz, F. A. A.; Trifonov, A.; Guerin, C. *Inorg. Chem.* **2008**, *47*, 775−777. (c) Kitagawa, S.; Kitaura, R.; Norc, S. *Angew. Chem., Int. Ed.* **2004**, *43*, 2334−2375. (d) Forster, P. M.; Eckert, J.; Heiken, B. D.; Parise, J. B.; Yoon, J. W.; Jhung, S. H.; Chang, J.-S.; Cheetham, A. K. *J. Am. Chem. Soc.* **2006**, *128*, 16846−16850. (e) Kar, P.; Guha, P. M.; Drew, M. G. B.; Ishida, T.; Ghosh, A. *Eur. J. Inorg. Chem.* **2011**, 2075−2085. (f) Kar, P.; Biswas, R.; Drew, M. G. B.; Ida, Y.; Ishida, T.; Ghosh, A. *Dalton Trans.* **2011**, *40*, 3295−3304. (g) Givaja, G.; Amo-Ochoa, P.; Gómez-García, C. J.; Zamora, F. *Chem. Soc. Rev.* **2012**, *41*, 115−157.

(2) (a) Zhou, A. J.; Qin, L. J.; Beedle, C. C.; Ding, S.; Nakano, M.; Leng, J. D.; Tong, M. L.; Hendrickson, D. N. *Inorg. Chem.* **2007**, *46*, 8111−8113. (b) Ge, C. H.; Cui, A. L.; Ni, Z. H.; Jiang, Y. B.; Zhang, L. F.; Ribas, J.; Kou, H. Z. *Inorg. Chem.* **2006**, *45*, 4883−4885. (c) Wang, M.; Ma, C.; Chen, C. *Dalton Trans.* **2008**, 4612−4620. (d) Yang, P. P.; Wang, X. L.; Li, L. C.; Liao, D. Z. *Dalton Trans.* **2011**, *40*, 4155−4161. (e) Ribas, J.; Escuer, A.; Monfort, M.; Vicente, R.; Cortes, R.; Lezama, L.; Rojo, T. *Coord. Chem. Rev.* **1999**, *193−195*, 1027−1068. (f) Chastanet, G.; Le Guennic, B.; Aronica, C.; Pilet, G.; Luneau, D.; Bonnet, M. L.; Robert, V. *Inorg. Chim. Acta* **2008**, *361*, 3847−3855. (g) Escuert, A.; Aromi, G. *Eur. J. Inorg. Chem.* **2006**, 4721−4736. (h) Adhikary, C.; Koner, S. *Coord. Chem. Rev.* **2010**, *254*, 2933−2958.

(3) (a) Nastase, S.; Tuna, F.; Maxim, C.; Muryn, C. A.; Avarvari, N.; Winpenny, R. E. P.; Andruh, M. *Cryst. Growth Des.* **2007**, *7*, 1825−1831. (b) Hewitt, I. J.; Tang, J. K.; Madhu, N. T.; Clerac, R.; Buth, G.; Anson, C. E.; Powell, A. K. *Chem. Commun.* **2006**, 2650−2652. (c) Mialane, P.; Duboc, C.; Marrot, J.; Riviere, E.; Dolbecq, A.; Secheresse, F. *Chem.—Eur. J.* **2006**, *12*, 1950−1959. (d) Mukherjee, S.; Gole, B.; Song, Y.; Mukherjee, P. S. *Inorg. Chem.* **2011**, *50*, 3621−3631. (e) Mukherjee, S.; Mukherjee, P. S. *Inorg. Chem.* **2010**, *49*, 10658−10667. (f) Mukherjee, S.; Gole, B.; Chakrabarty, R.; Mukherjee, P. S. *Inorg. Chem.* **2009**, *48*, 11325−11334.

(4) (a) Mialane, P.; Dolbecq, A.; Marrot, J.; Riviere, E.; Secheresse, F. *Chem.—Eur. J.* **2005**, *11*, 1771−1778. (b) Goher, M. A. S.; Cano, J.; Journaux, Y.; Abu-Youssef, M. A. M.; Mautner, F. A.; Escuer, A.; Vicente, R. *Chem.—Eur. J.* **2000**, *6*, 778−784. (c) Ribas, J.; Montfort, M.; Solans, X.; Drillon, M. *Inorg. Chem.* **1994**, *33*, 742−745. (d) Papaefstathiou, G. S.; Perlepes, S. P.; Escuer, A.; Vicente, R.; Font-Bardia, M.; Solans, X. *Angew. Chem., Int. Ed.* **2001**, *40*, 884−886. (e) Meyer, F.; Kircher, P.; Pritzkow, H. *Chem. Commun.* **2003**, 774−775.

(5) (a) Agnus, Y.; Lewis, R.; Gisselbrecht, J. P.; Weiss, R. *J. Am. Chem. Soc.* **1984**, *106*, 93−102. (b) Mckee, V.; Zvagulis, M.; Dagdigian, J. V.; Patch, M. G.; Reed, C. A. *J. Am. Chem. Soc.* **1984**, *106*, 4765−4772.

(6) (a) Kahn, O.; Sikorav, S.; Gouteron, J.; Jeannin, S.; annin, Y. J. *Inorg. Chem.* **1983**, *22*, 2877−2883. (b) Comarmond, P.; Plumere, P.;

Lehn, J. M.; Augus, Y.; Louis, R.; Weiss, R.; Kahn, O.; Morgenstern-Badarau, I. *J. Am. Chem. Soc.* **1982**, *104*, 6330−6340. (c) Waksman, I. B.; Boillot, M. L.; Kahn, O.; Sikorov, S. *Inorg. Chem.* **1984**, *23*, 4454−4459.
(7) (a) Saha, S.; Koner, S.; Tuchagues, J.-P.; Boudalis, A. K.; Okamoto, K.-I.; Mal, D. *Inorg. Chem.* **2005**, *44*, 6379−6385. (b) Ray, M. S.; Ghosh, A.; Bhattacharya, R.; Mukhopadhyay, G.; Drew, M.G. B.; Ribas, J. *Dalton Trans.* **2004**, 252−259. (c) Ray, M. S.; Ghosh, A.; Chaudhuri, S.; Drew, M. G. B.; Ribas, J. *Eur. J. Inorg. Chem.* **2004**, 3110−3117. (d) Liu, T.; Wang, Y.-F.; Wang, Z.-M.; Gao, S. *Chem.—Asian J.* **2008**, *3*, 950−957.
(8) (a) Ribas, J.; Monfort, M.; Diaz, C.; Bastos, C.; Solans, X. *Inorg. Chem.* **1994**, *33*, 484−489. (b) Cortes, R.; Lezama, L.; Pizarro, J. L.; Arriortua, M. I.; Solans, X.; Rojo, T. *Angew. Chem., Int. Ed. Engl.* **1994**, *33*, 2488−2489. (c) Ribas, J.; Monfort, M.; Resino, I.; Solans, X.; Rabu, P.; Maingot, F.; Drillon, M. *Angew. Chem., Int. Ed. Engl.* **1996**, *35*, 2520−2522. (d) Tang, L.-F.; Zhang, L.; Li, L.-C.; Cheng, P.; Wang, Z.-H.; Wang, J.-T. *Inorg. Chem.* **1999**, *38*, 6326−6328. (e) Abu-Youssef, M. A.; Escuer, A.; Gatteschi, D.; Goher, M. A. S.; Mautner, F. A.; Vicente, R. *Inorg. Chem.* **1999**, *38*, 5716−5723. (f) Abu-Youssef, M.; Escuer, A.; Goher, M. A. S.; Mautner, F. A.; Vicente, R. *Eur. J. Inorg. Chem.* **1999**, 687−691. (g) Goher, M. A. S.; Al-Salem, N. A.; Mautner, F. A. *J. Coord. Chem.* **1998**, *44*, 119−131. (h) Triki, S.; Gómez-García, C. J.; Ruiz, E.; Sala-Pala, J. *Inorg. Chem.* **2005**, *44*, 5501−5508.
(9) (a) Kar, P.; Haldar, R.; Gómez-García, C. J.; Ghosh, A. *Inorg. Chem.* **2012**, *51*, 4265−4273. (b) Ovcharenko, V.; Fursova, E.; Romanenko, G.; Ikorskii, V. *Inorg. Chem.* **2004**, *43*, 3332−3334. (c) Kar, P.; Biswas, R.; Ida, Y.; Ishida, T.; Ghosh, A. *Cryst. Growth Des.* **2011**, *11*, 5305−5315.
(10) (a) Hou, H.; Wei, Y.; Fan, Y.; Du, C.; Zhu, Y.; Song, Y.; Niu, Y.; Xin, X. *Inorg. Chim. Acta* **2001**, *319*, 212−218. (b) Zhao, Q. H.; Liu, Y. Q.; Fang, R. B. *Inorg. Chem. Commun.* **2006**, *9*, 699−702. (c) Ghosh, A. K.; Ghoshal, D.; Zangrando, E.; Ribas, J.; Ray Chaudhuri, N. *Inorg. Chem.* **2005**, *44*, 1786−1793. (d) Ni, Z.-H.; Kou, H.-Z.; Zheng, L.; Zhao, Y.-H.; Zhang, L.-F.; Wang, R.-J.; Cui, A.-L.; Sato, O. *Inorg. Chem.* **2005**, *44*, 4728−4736.
(11) (a) Han, S. J.; Manson; Kim, L. J.; Miller, J. S. *Inorg. Chem.* **2000**, *39*, 4182−4185. (b) Escuer, A.; Vicente, R.; Goher, M. A. S.; Mautnero, F. A. *Inorg. Chem.* **1995**, *34*, 5707−5708. (c) Ma, B.-Q.; Sun, H.-L.; Gao, S.; Su, G. *Chem. Mater.* **2001**, *13*, 1946−1948. (d) Gao, E.-Q.; Wang, Z.-M.; Yan, C.-H. *Chem. Commun.* **2003**, 1748−1749. (e) Escuer, A.; Vicente, R.; Goher, M. A. S.; Mautner, F. A. *J. Chem. Soc., Dalton Trans.* **1997**, 4431−4434. (f) Cano, J.; Journaux, Y.; Goher, M. A. S.; Abu-Youssef, M. A. M.; Mautner, F. A.; Reib, G. J.; Escuer, A.; Vicente, R. *New J . Chem.* **2005**, *29*, 306−314. (g) Escuer, A.; Mautner, F.; A. Goher, M. A. S.; Abu-Youssef, M. A. M.; Vicente, R. *Chem. Commun.* **2005**, 605−607.
(12) (a) Brown, E. V.; Granneman, G. R. *J. Am. Chem. Soc.* **1975**, *97*, 621−627. (b) Dinolfo, P. H.; Williams, M. E.; Stern, C. L.; Hupp, J. T. *J. Am. Chem. Soc.* **2004**, *126*, 12989−13001.
(13) *SHELXS97* and *SHELXL97*, programs for crystallographic solution and refinement. Sheldrick, G. M. *Acta Crystallogr.* **2008**, *A64*, 112.
(14) *CrysAlis*; Oxford Diffraction Ltd.: Abingdon, U.K., 2006.
(15) (a) *SAINT, version 6.02, SADABS, version 2.03*; Bruker AXS, Inc.: Madison, WI, 2002. (b) *ABSPACK*; Oxford Diffraction Ltd: Oxford, U.K., 2005.
(16) (a) Sarkar, B.; Konar, S.; Gomez-Garcia, C.; J. Ghosh, A. *Inorg. Chem.* **2008**, *47*, 11611−11619. (b) Chattopadhyay, S.; Ray, M. S.; Drew, M. G.B.; Figuerola, A.; Diaz, C.; Ghosh, A. *Polyhedron* **2006**, *25*, 2241−2253.
(17) Escuer, A.; Vicente, R.; Goher, M. A. S.; Mautner, F. A.; Abu-Youssef, M. A. M. *Chem. Commun.* **2002**, 64−65.
(18) (a) Martin, S.; Barandika, M. G.; Lezama, L.; Pizarro, J. L.; Serna, Z. E.; de Larramendi, J. I. R.; Arriortua, M. I.; Rojo, T.; Cortes, R. *Inorg. Chem.* **2001**, *40*, 4109−4115. (b) Liu, C.-M.; Yu, Z.; Xiong, R.-G.; Liu, K.; You, X.-Z. *Inorg. Chem. Commun.* **1999**, *2*, 31−34.
(19) Gao, E.-Q.; Cheng, A.-L.; Xu, Y.-X.; He, M.-Y.; Yan, C.-H. *Inorg. Chem.* **2005**, *44*, 8822−8835.
(20) Wang, X.-Y.; Wang, L.; Wang, Z.-M.; Su, G.; Gao, S. *Chem. Mater.* **2005**, *17*, 6369−6380.
(21) Li, X.-B.; Ma, Y.; Zhang, X.-M.; Zhang, J.-Y.; Gao, E.-Q. *Eur. J. Inorg. Chem.* **2011**, 4738−4744.
(22) Munno, G. D.; Julve, M.; Viau, G.; Lloret, F.; Faus, J.; Viterbo, D. *Angew. Chem., Int. Ed. Engl.* **1996**, *35*, 1807−1809.
(23) (a) Youssef, M. A.; Escuer, A.; Goher, M. A. S.; Mautner, F. A.; Vicente, R. *J. Chem. Soc., Dalton Trans.* **2000**, 413−416. (b) Gao, E.-Q.; Bai, S.-Q.; Wang, Z.-M.; Yan, C.-H. *J. Am. Chem. Soc.* **2003**, *125*, 4984−4985. (c) Shen, Z.; Zuo, J.-L.; Yu, Z.; Zhang, Y.; Bai, J.-F.; Che, C.-M.; Fun, H.-K.; Vittal, J. J.; You, X.-Z. *J. Chem. Soc., Dalton Trans.* **1999**, 3393−3398. (d) Jia, Q.-X.; Tian, H.; Zhang, J.-Y.; Gao, E.-Q. *Chem.—Eur. J.* **2011**, *17*, 1040−1051.
(24) Lines, M. E. *J. Phys. Chem. Solids.* **1970**, *31*, 101−116.
(25) Fisher, M. E. *Am. J. Phys.* **1964**, *32*, 343−346.
(26) Connor, O. C. J. *Prog. Inorg. Chem.* **1982**, *29*, 203−283.
(27) (a) Escuer, A.; Vicente, R.; Goher, M. A. S.; Mautner, F. A. *Inorg. Chem.* **1996**, *35*, 6386−6391. (b) Escuer, A.; Vicente, R.; Goher, M. A. S.; Mautner, F. A. *Inorg. Chem.* **1998**, *37*, 782−787. (c) Cortés, R.; Drillon, M.; Solans, X.; Lezama, L.; Rojo, T. *Inorg. Chem.* **1997**, *36*, 677−683.
(28) Gao, E.-Q.; Yue, Y.-F.; Bai, S.-Q.; He, Z.; Yan, C.-H. *J. Am. Chem. Soc.* **2004**, *126*, 1419−1429.
(29) Ruiz, E.; Cano, J.; Alvarez, S.; Alemany, P. *J. Am. Chem. Soc.* **1998**, *120*, 11122−11129.